

## Synthesis, Enantiomeric Conformations, and Stereodynamics of Aromatic *ortho*-Substituted Disulfones

by Jérôme Lacour<sup>\*a)</sup>, David Monchaud<sup>a)</sup>, Jiri Mareda<sup>a)</sup>, France Favarger<sup>a)</sup>, and Gérard Bernardinelli<sup>b)</sup>

<sup>a)</sup> Département de Chimie Organique, Université de Genève, quai Ernest-Ansermet 30, CH-1211 Geneva 4

<sup>b)</sup> Laboratoire de Cristallographie, Université de Genève, quai Ernest-Ansermet 24, CH-1211 Geneva 4

---

Aromatic *ortho*-disulfone derivatives are readily accessible from diiodide precursors by Cu<sup>I</sup>-mediated reaction with sodium sulfinate salts (DMF, 110°). The sulfonyl substituents adopt in solution and in the solid state two enantiomeric conformations ( $\lambda$  and  $\delta$ ) as evidenced by <sup>31</sup>P- and <sup>1</sup>H-NMR data of the chiral *D*<sub>3</sub>-symmetric tris[4,5-bis(4-methylphenyl)sulfonyl]benzene-1,2-diolato(2-)- $\kappa$ O, $\kappa$ O' phosphate(v) anion (**3a**) and 1,2-bis(camphor-10-sulfonyl)-4,5-dimethoxybenzene ((=1,2-bis{[(1*S*,4*R*)-7,7-dimethyl-2-oxobicyclo[2.2.1]hept-1-yl]methyl}sulfonyl)-4,5-dimethoxybenzene; **6c**). X-Ray structure analysis of 1,2-dimethoxy-4,5-bis(methylsulfonyl)benzene (**6a**) and 1,2-dimethoxy-4,5-bis(4-methylphenyl)sulfonyl]benzene (**6b**) confirmed in the solid state the preferred chiral orientation of the sulfonyl groups. Dynamic conformational isomerism was detected for **6c** in its <sup>1</sup>H-NMR in the temperature range of 110°, the corresponding free energy being 19.8 kcal·mol<sup>-1</sup>.

---

**Introduction.** – The octahedral geometry of a pentavalent hexacoordinated P-atom allows the formation of chiral phosphate anions –  $\Delta$  and  $\Lambda$  enantiomers – by complexing the P-atom with three identical symmetrical bidentate ligands [1]. Hexacoordinated tris(benzenediolato)phosphate anion **1**, of particular interest for its easy preparation from pyrocatechol (= benzene-1,2-diol), PCl<sub>5</sub>, and an amine, is unfortunately configurationally labile as an ammonium salt in solution due to an acid-induced racemization mechanism [2]. Recently, we reported that the introduction of electron-withdrawing groups (Cl-atoms) at the aromatic rings increases the configurational stability of the resulting tris(tetrachlorobenzenediolato)phosphate(v) – (= TRISPHAT) derivative **2** (Fig. 1). This anion can be resolved associated with a chiral ammonium cation. It is an efficient NMR chiral shift reagent, a powerful resolving agent for ruthenium(II) complexes, and a chiral inducer onto iron(II) tris(diimine) compounds [3].

To extend the pool of chiral anions to choose from for possible asymmetric applications, we decided to prepare novel hexacoordinated phosphate anions derived from new electron-deficient pyrocatechols. We decided to focus on the synthesis of pyrocatechol derivatives substituted with strong electron-withdrawing groups, such as the sulfonyl groups MeSO<sub>2</sub> and *p*-TolSO<sub>2</sub> [4]. The new pyrocatechols should be at least as electron-poor as tetrachloropyrocatechol, and literature precedents convinced us of the need to introduce at least two sulfonyl substituents [4]. The pattern of distribution of the two electron-withdrawing groups on the pyrocatechols was also essential. Asymmetrically substituted pyrocatechols would lead – in octahedral geometry – to the synthesis of meridional and facial isomers of the phosphate anions. The two

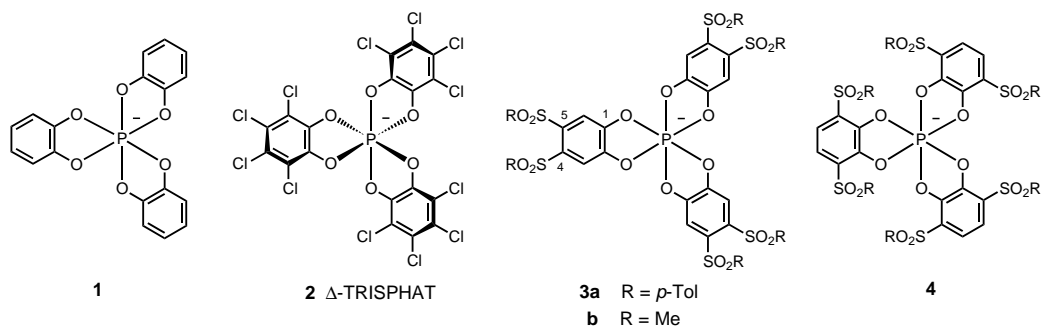


Fig. 1. Hexacoordinated phosphate anions: **1**, **2** (TRISPHAT), **3**, and **4**

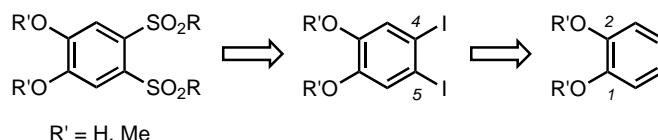
symmetrical 4,5- and 3,6-disubstitutions were then compatible with the making of  $D_3$ -symmetric anions of the general structures **3** and **4** (Fig. 1).

Herein, we report that the introduction of sulfonyl substituents at C(4) and C(5) of the pyrocatechol ligand led to mixtures of diastereoisomeric hexacoordinated phosphate anions **3**. This is due to the adoption of enantiomeric conformations ( $\delta$  and  $\lambda$ ) by each pair of the *ortho*-positioned sulfonyl groups. To demonstrate further this effect and characterize the slow interconversion between the  $\delta$  and  $\lambda$  forms, enantiomerically pure 1,2-bis(camphor-10-sulfonyl)-4,5-dimethoxybenzene (**6c**) was prepared.

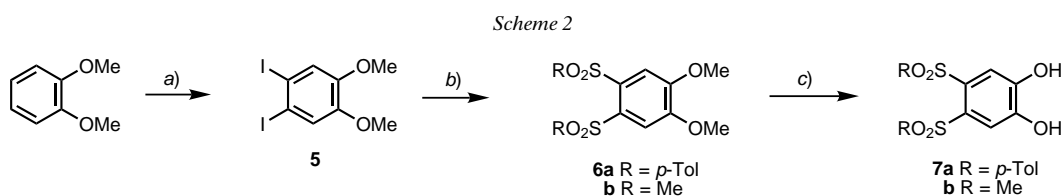
**2. Results and Discussion.** – 2.1. *Syntheses of 4,5-Bis(sulfonyl)pyrocatechols.* Of the two symmetrical modes of disubstitution in agreement with the making of  $D_3$ -symmetric anions, a simple retrosynthetic analysis led us to tackle first the synthesis of 4,5-disubstituted derivatives (Scheme 1). Recently, Suzuki *et al.* reported a simple and high-yielding route to aromatic sulfones by a  $\text{Cu}^{\text{I}}$ -mediated reaction of aryl iodides with aromatic sodium sulfinates [5]. No *ortho*-diiodobenzene derivatives had been tested. However, the generality of this reaction made us confident that we could use it to introduce the two *ortho*-positioned sulfonyl groups. Furthermore, literature precedents indicated that 4,5-diiodoveratrol (=1,2-diiodo-4,5-dimethoxybenzene; **5**) could be prepared in a single step from veratrol with a combination of iodine and periodic acid, compound **5** being an ideal starting material [6].

We decided to attempt the sulfonylation reaction under reported conditions with commercially available sodium *p*-toluenesulfinate (=sodium 4-methylbenzenesulfinate). We also extended the coupling methodology to the readily prepared methanesulfinate derivative [7]. As reported, diiodination of veratrol with  $\text{I}_2/\text{H}_5\text{IO}_6$  proceeded smoothly to give **5** in 83% yield (Scheme 2). Bis-sulfonylation of **5** resulted, after optimization, in the syntheses of **6a** (R = *p*-Tol; 88%) and **6b** (R = Me; 95%) with high yields. The  $\text{Cu}^{\text{I}}$ -mediated coupling can thus be applied with either aromatic and aliphatic sulfinates. Longer reaction times (> 64 h) were required for the double sulfonylation. Prolonged heating at higher temperatures (125°) led to lower amounts of bis-sulfonylated derivatives.  $^1\text{H}$ - and  $^{13}\text{C}$ -NMR analyses of **6a,b** did not reveal any particularity, except for a signal broadening that could only be understood in the course of this study. Simple deprotection of the methylated derivatives **6a,b** under classical

Scheme 1. Retrosynthetic Scheme for the Synthesis of 4,5-Bis(sulfonyl)pyrocatechol Derivatives



conditions ( $\text{BBr}_3$ ,  $\text{CH}_2\text{Cl}_2$ ) led to the 4,5-bis(*p*-tolylsulfonyl)pyrocatechol (**7a**) and 4,5-bis(methylsulfonyl)pyrocatechol (**7b**) in 93 and 100% yield, respectively (Scheme 2) [8]. The reaction of **7a** required more elevated temperature ( $45^\circ$  instead of  $24^\circ$ ) to proceed with high yield.

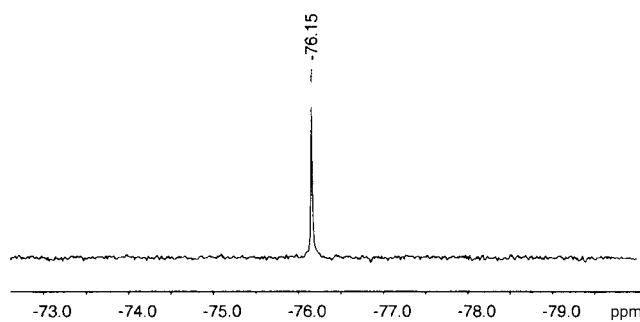
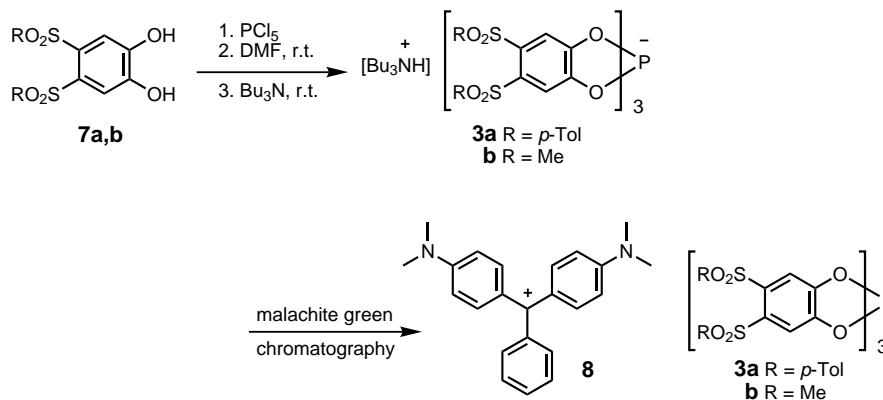
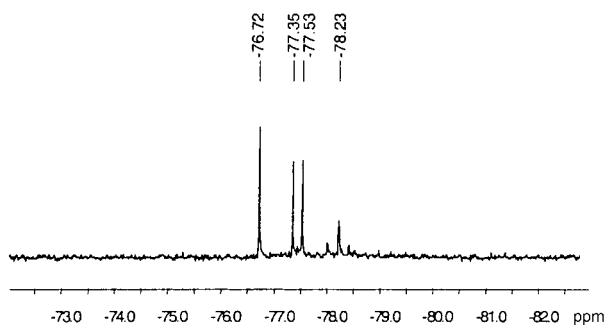


a)  $\text{I}_2$ ,  $\text{H}_5\text{IO}_6$ , MeOH,  $70^\circ$ ; **5** (83%). b) CuI,  $\text{RSO}_2\text{Na}$  (3.0 equiv.), DMF,  $110^\circ$ ; **6a** (R = *p*-Tol, 88%) and **6b** (R = Me, 95%). c)  $\text{BBr}_3$  (5.0 equiv.),  $\text{CH}_2\text{Cl}_2$ ; **7a** (R = *p*-Tol; 93%) and **7b** (R = Me, 100%).

### 2.2. Syntheses of Tris[4,5-bis(sulfonyl)benzenediolato]phosphate Anions **3a** and **3b**.

The syntheses of the corresponding hexacoordinated phosphate anions were first attempted under conditions developed in our laboratory for the synthesis of TRISPHAT **2**. However, reactions of **7a** or **7b** and  $\text{PCl}_5$  in toluene and addition of  $\text{Bu}_3\text{N}$  in  $\text{CH}_2\text{Cl}_2$  did not yield the desired  $(\text{Bu}_3\text{NH}) \cdot \mathbf{3a}$  and  $(\text{Bu}_3\text{NH}) \cdot \mathbf{3b}$  salts.  $^{31}\text{P}$ -NMR Analyses of the crude reaction mixtures revealed signals between 0 and 5 ppm corresponding to classical tetraordinated phosphate derivatives. Assuming that this failure was the result of poor solubility in toluene of pyrocatechols **7a,b** and/or the resulting P-derivatives, we circumvented the problem by choosing more-polar solvent conditions. Addition of  $\text{PCl}_5$  to solutions of the pyrocatechols in  $\text{CH}_2\text{Cl}_2$  (**7a**) or MeCN (**7b**), then reaction, and addition of  $\text{Bu}_3\text{N}$  in DMF afforded the desired  $(\text{Bu}_3\text{NH}) \cdot \mathbf{3a}$  and  $(\text{Bu}_3\text{NH}) \cdot \mathbf{3b}$  salts along with minor amounts of degradation products (Scheme 3). Purification of the crude mixtures could be effected by metathesis reactions with malachite green oxalate and chromatography ( $\text{SiO}_2$ ) to afford the bis [4-(dimethylamino)phenyl]phenylmethylium (**8**) salts, *i.e.*, **8**·**3a** and **8**·**3b**, in 63 and 82% yield, respectively (over two steps and nonoptimized).

2.3.  $^{31}\text{P}$ -NMR Analysis: Multiple Isomers for Anion **3a**. Characterization of salt **8**·**3b** by  $^{31}\text{P}$ -NMR revealed one signal corresponding to the hexacoordinated phosphate anion **3b** ( $(\text{D})_6$ acetone,  $\delta -76.2$ , Fig. 2). However,  $^{31}\text{P}$ -NMR analysis of **8**·**3a** was, at first glance, somewhat puzzling. Four signals were observed – while only one was expected – in the  $-80$  ppm region characteristic of the tris(benzenediolato)phosphate anions ( $(\text{D})_6$ DMSO;  $\delta -76.7$ ,  $-77.3$ ,  $-77.5$ , and  $-78.2$ , Fig. 3). This result was furthermore surprising as only one set of signals corresponding to anion **3a** could be observed in the  $^1\text{H}$ -NMR spectrum. Further characterization of salt **8**·**3a** by mass spectrometry (ES-MS) confirmed its structural integrity. The four signals in the  $^{31}\text{P}$ -

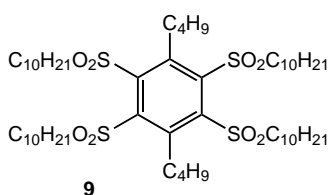
Scheme 3. *Synthesis and Isolation of Hexacoordinated Phosphate Anions 3a and 3b*Fig. 2. *Partial  $^{31}\text{P}$ -NMR spectrum ((D<sub>6</sub>)acetone, 162 MHz) of 8·3b*Fig. 3. *Partial  $^{31}\text{P}$ -NMR spectrum ((D<sub>6</sub>)DMSO; 162 MHz) of 8·3a*

NMR spectrum could not be explained by the presence of four different chemical compounds. The easiest means to explain the four signals was to consider that anion **3a** exists in four diastereoisomeric forms.

2.4. *Hypothetical Enantiomeric Conformations for 4,5-Bis(sulfonyl)pyrocatechols.* The observation of four stereoisomers for **3a** was somewhat reminiscent of what is

usually noticed for tris(bidentate) octahedral complexes made of nonplanar chelate rings, such as  $[\text{Co}(\text{en})_3]^{3+}$  (en = ethane-1,2-diamine). As first noted by *Corey* and *Bailar*, when chelate rings adopt chiral conformations ( $\delta$  and  $\lambda$ ), four diastereoisomers – always appearing in enantiomer pairs – are generated due to the inherent chirality of the octahedral complexes ( $\Delta$  and  $\Lambda$ ):  $\Delta(\delta\delta\delta)/\Lambda(\lambda\lambda\lambda)$ ,  $\Delta(\delta\delta\lambda)/\Lambda(\lambda\lambda\delta)$ ,  $\Delta(\delta\lambda\lambda)/\Lambda(\lambda\delta\delta)$ ,  $\Delta(\lambda\lambda\lambda)/\Lambda(\delta\delta\delta)$  [9][1]. However, the planarity of the chelating pyrocatechol rings in **3a** was not compatible with such an explanation. If chiral conformations were to be the source of the four signals observed in the  $^{31}\text{P}$ -NMR spectrum, they would have to result from the spatial arrangement of the sulfonyl substituents.

We turned our attention to the work of *Collard* and co-workers [10]. In 1995, they reported the synthesis of highly twisted substituted arenes of the general 1,4-dialkyl-2,3,5,6-tetra(alkylsulfonyl)benzene skeleton (e.g., **9**). In these compounds, X-ray structural analysis showed that the *ortho*-positioned sulfonyl groups adopt an alternating orientation, and the rings are highly twisted with external torsion angles of  $46^\circ$ . *Collard* and co-workers also observed dynamic NMR behavior corresponding to a slow isomerism of the sulfonyl side chains (barrier of interconversion of ca.  $17 \text{ kcal} \cdot \text{mol}^{-1}$ ).



2.5. *Solid-State Analysis of 4,5-Bis(p-tolylsulfonyl)veratrol 6a and 4,5-Bis(methylsulfonyl)veratrol 6b*. X-Ray structural analyses of crystals of **6a**<sup>1)</sup> and **6b** were undertaken and confirmed the existence of an ‘up-and-down’ arrangement of the *ortho*-positioned sulfonyl groups in the solid state (Figs. 4 and 5). In both compounds, the sulfonyl groups are twisted around a pseudo- $C_2$  axis passing through the midpoint of the C(1)–C(2) and C(4)–C(5) bonds. The S–C–C–S torsional angles are close to  $0^\circ$  ( $3.4(6)^\circ$  and  $-2.0(6)^\circ$  and **6a** and **6b**, resp.) meaning a quasi-planar pyrocatechol ring contrary to what was observed by *Collard* and co-workers [10]. The crystal structures of **6a** and **6b** being centrosymmetric, both  $\delta$  and  $\lambda$  configurations were observed in the solid state. The molecular packing of **6b** shows stacking interactions of the pyrocatechol rings (Fig. 6) on both sides of inversion centres and running along the [100] direction (interplane distances:  $3.481(9)$  and  $3.527(9)$  Å).

2.6. *Synthesis, Diastereoisomeric Conformations, and Stereodynamics of the 4,5-Bis(camphor-10-sulfonyl)veratrol (6c)*. To demonstrate in solution the presence of these enantiomeric  $\delta$  and  $\lambda$  conformations, we decided to study a model compound which would be easily accessible following the synthetic route already established and whose conformational isomerism could be determined by  $^1\text{H}$ -NMR. The observation of

<sup>1)</sup> The present report follows a previous communication of our group, which described the structure of **6a** in detail (CCD refcode: qoycuc) [11].

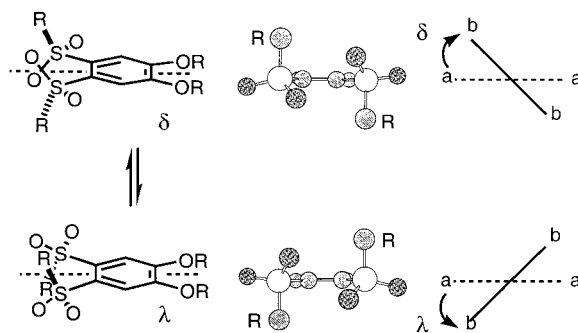


Fig. 4. Views of the conformations adopted by ortho-positioned sulfonyl groups and configurational assignment ( $\delta$  and  $\lambda$ ). a·····a constitutes the plane of the phenyl ring, and b·····b represents the line passing through the R substituents.

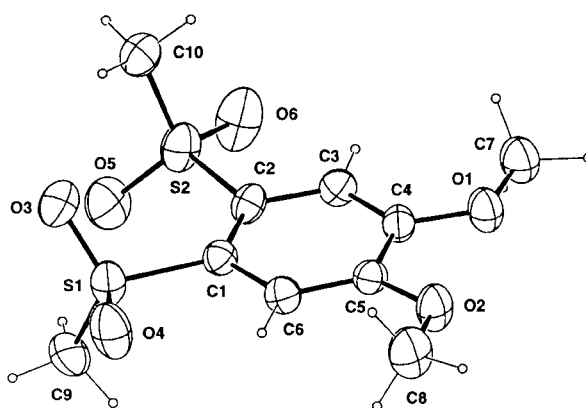


Fig. 5. ORTEP View of **6b** ( $\delta$  configuration) with the atom numbering. Ellipsoids are represented with 40% probability level. Selected torsional angles [ $^\circ$ ]: C(3)–C(4)–O(1)–C(7) =  $-4.7(6)$ , C(6)–C(5)–O(2)–C(8) =  $-9.3(6)$ , C(2)–C(1)–S(1)–C(9) =  $74.2(4)$ , and C(1)–C(2)–S(2)–C(10) =  $79.8(4)$ .

the enantiomeric  $\delta$  and  $\lambda$  conformations necessitates the presence of another stereogenic element, and the introduction of a chiral probe was thus mandatory. The rapid access to the enantiomerically pure sodium camphor-10-sulfinate salt **10** from the (+)-camphor-10-sulfonyl chloride led us to consider the synthesis of the derived 4,5-bis(camphor-10-sulfonyl)veratrol (**6c**). Chiral  $C_2$ -symmetric compound **6c** would fit perfectly the above-mentioned criteria.

The synthesis of **6c** from diiodoveratrol **5** turned out to be more challenging than those of **6a** and **6b** (Scheme 4). Sulfinate salt **10** was unstable and decomposed (IR monitoring) slowly at room temperature even under inert conditions ( $N_2$ ). A large excess of **10** (25 equiv.) and longer reaction times were required for the  $Cu^I$ -mediated bis(sulfonylation) reaction to proceed with good yield (85%).  $^1H$ -NMR Analysis of **6c** at room temperature revealed as expected two sets of signals corresponding to the diastereoisomeric  $\delta$  and  $\lambda$  conformations. The diastereotopic protons  $CH_2(10)$  (Fig. 7)

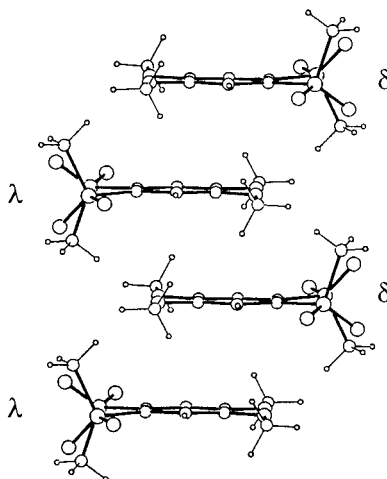
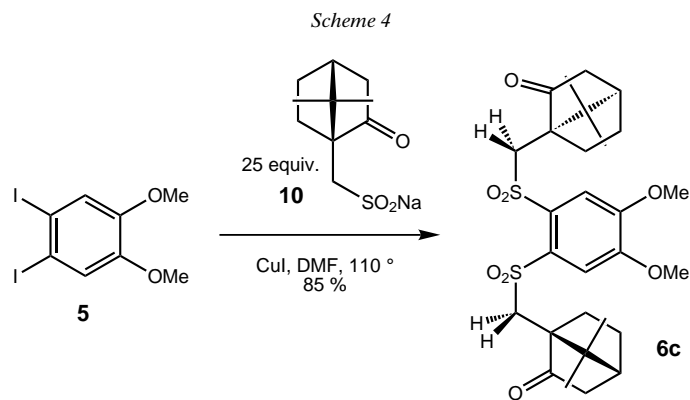


Fig. 6. Perspective view of the crystal packing of **6b** along the [100] direction showing the alternate stacking interactions of  $\lambda$  and  $\delta$  configurations

and the geminal Me groups of the camphorsulfonyl units gave rise to split signals, as well did the aromatic protons H–C(3') and the MeO groups of the veratrol ring (*Table*). The two diastereoisomeric  $\delta$  and  $\lambda$  conformations in **6c** are not identically populated as the integration of the respective signals revealed a 2.25 : 1 diastereomer ratio. Thus, the chiral camphorsulfonyl units lead not only to the magnetic non-equivalency of diastereoisomeric conformations but also to an asymmetric induction in favor of one of the configurations<sup>2)</sup>.

Dynamic conformational isomerism was detected for **6c** in the <sup>1</sup>H-NMR spectrum in a temperature range of 110° (*Fig. 8*), demonstrating without ambiguity the slow interconversion at room temperature between diastereoisomeric  $\delta$  and  $\lambda$  conformations



<sup>2)</sup> No attempts were made to determine which of the two diastereoisomeric conformations is preferred.

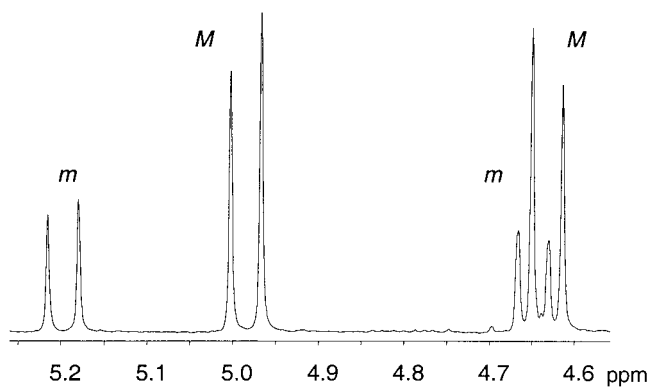


Fig. 7. Partial  $^1\text{H-NMR}$  spectrum (400 MHz,  $\text{CDCl}_3$ ) of **6c**. Methylene protons  $\text{CH}_2(10)$  of the major (*M*) and minor (*m*) diastereoisomeric conformations  $\delta$  or  $\lambda^2$ .

Table.  $^1\text{H-NMR}$  Chemical Shifts (400 MHz,  $\text{CDCl}_3$ ) for Selected Protons of the Major (*M*) and Minor (*m*) Diastereoisomeric Conformations of **6c**<sup>2</sup>)

	<i>m</i>	<i>M</i>
H-C(3')	8.29	8.20
H-C(10)	5.19, 4.64	4.98, 4.63
MeO	3.16	3.28
Me	1.04, 0.91	1.05, 0.90

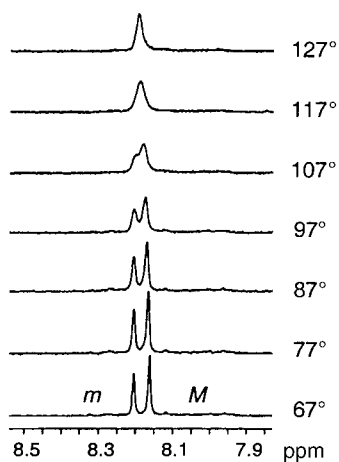
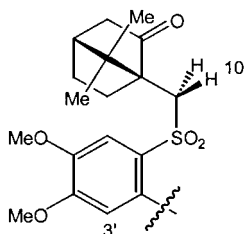


Fig. 8. Variable-temperature  $^1\text{H-NMR}$  measurements (400 MHz,  $(\text{D}_6)$ DMSO) of **6c**. H-C(3') signal of the major (*M*) and minor (*m*) diastereoisomeric conformations  $\delta$  and  $\lambda^2$ .



of aromatic *ortho*-disulfones. The corresponding free energy of interconversion is *ca.* 19.8 kcal · mol<sup>-13</sup>).

2.7. *Diastereoisomeric Conformations of Tris(4,5-bis(sulfonyl)benzenediolato)phosphate Anions.* Taking thus into account the existence – in the solid state and in solution – of enantiomeric  $\delta$  and  $\lambda$  conformations of the *ortho*-disulfones of each of the three chelating pyrocatechols, four diastereoisomers – always appearing in enantiomer pairs – can be considered for anions **3a** and **3b**:  $\Delta(\delta\delta\delta)/\Lambda(\lambda\lambda\lambda)$ ,  $\Delta(\delta\delta\lambda)/\Lambda(\lambda\lambda\delta)$ ,  $\Delta(\delta\lambda\lambda)/\Lambda(\lambda\delta\delta)$ , and  $\Delta(\lambda\lambda\lambda)/\Lambda(\delta\delta\delta)$ . Two of the four diastereoisomers of anion **3b** are depicted in Fig. 9, wherein the orientation of the sulfonyl groups determined by the X-ray structural analysis is used<sup>4</sup>). For anion **3a**, diastereoisomers  $\Delta(\delta\delta\delta)$  and  $\Delta(\lambda\lambda\lambda)$  are represented in Fig. 10, wherein a geometry calculated by molecular mechanics (MM+) was used for the sulfonyl groups<sup>5</sup>).

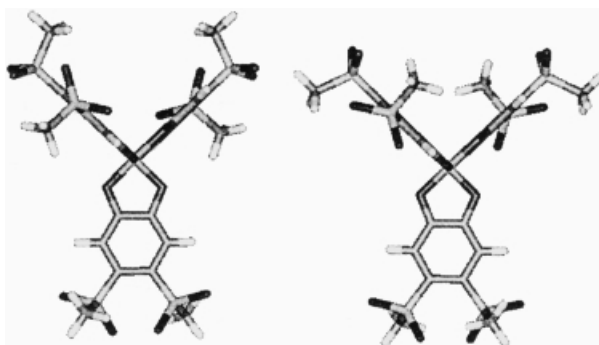


Fig. 9. Views (Chem3D) of two diastereoisomers of **3b** ( $\Delta(\delta\delta\delta)$  and  $\Delta(\lambda\lambda\lambda)$ )

For anion **3a**, each of the signals observed in the <sup>31</sup>P-NMR spectrum can thus be assigned to one of the diastereoisomers considering that the rate of interconversion of the *p*-tolylsulfonyl groups is slow compared to the NMR time scale. A stereodynamic study was attempted by variable-temperature <sup>31</sup>P-NMR measurements. Within the range of temperature studied (25–147°), no coalescence of the four signals was observed, showing an even slower equilibration of the  $\delta$  and  $\lambda$  conformations than for **6c**<sup>6</sup>). Unfortunately, degradation of anion **3a** occurred at high temperature – most probably through an acid-catalyzed decomposition pathway – limiting the scope of this investigation (Fig. 11)<sup>7</sup>).

<sup>3</sup>) The relationship  $\Delta G^\ddagger = RT_c (22.96 + \ln(T_c/\Delta\nu))$  was used to determine the activation energy  $\Delta G^\ddagger$  from the coalescence temperature  $T_c$  [K] and the frequency separation of the peaks  $\Delta\nu$  [Hz].

<sup>4</sup>) No calculations have been attempted on those structures.

<sup>5</sup>) Hyperchem 5.0, HyperCube Inc., 1996.

<sup>6</sup>) The activation energy  $\Delta G^\ddagger$  is higher than 21.4 kcal · mol<sup>-1</sup>, considering a  $T_c \geq 147^\circ$  and a minimum  $\Delta\nu$  value of 29 Hz ( $\Delta\delta = -77.35$  to  $-77.53$ ).

<sup>7</sup>) Dynamic conformational isomerism was not detected for **3a** in the <sup>31</sup>P-NMR spectrum at 147°, the corresponding free energy is thus higher than 19.5 kcal · mol<sup>-1</sup>.

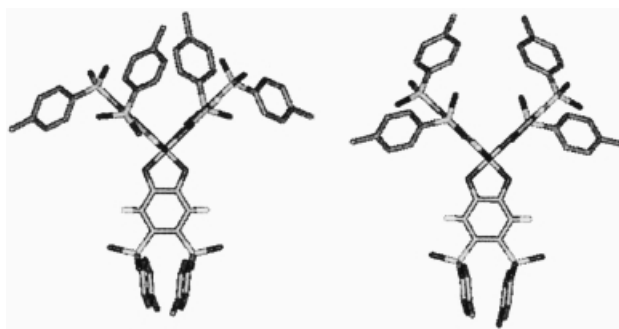


Fig. 10. Views (Chem3D) of two diastereoisomers of **3a** ( $\Delta(\delta\delta\delta)$  and  $\Delta(\lambda\lambda\lambda)$ )

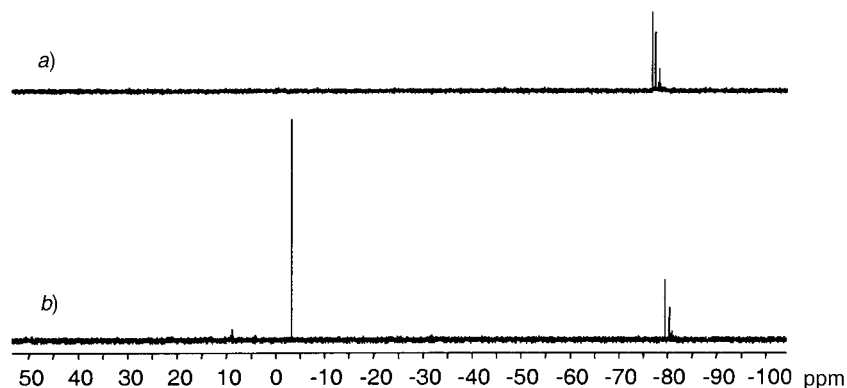


Fig. 11. Partial <sup>31</sup>P-NMR spectrum (162 MHz, DMSO) of salt **8·3a** a) before and b) after heating at 147°

For anion **3b**, two explanations can be proposed to rationalize the observation of a single signal in the <sup>31</sup>P-NMR spectrum. The four diastereoisomers are either isochronous or the rate of interconversion between the  $\delta$  and  $\lambda$  conformations is rapid compared to the NMR time scale, the first explanation being more likely than the second. The smaller size of the methylsulfonyl groups – compared to the *p*-tolylsulfonyl – induce probably less strain between the adjacent chelating pyrocatechol rings of the four diastereoisomers, and identical <sup>31</sup>P-NMR chemical shifts for the four derivatives is understandable.

2.8. *Computational Studies of the 4,3-Bis(sulfonyl)arenes.* To gain insight into the rate of conversion for 4,5-bis(sulfonyl)veratrols, we have performed quantum-chemical computations for the barrier to internal rotation of sulfonyl groups in the model compound: 4,5-bis(methylsulfonyl)veratrol (**6b**). The computations at the B3LYP level [12] and the 3-21G basis set [13] as implemented within the Gaussian 98 package [14] were used for the geometry optimizations of local minima. The structures of 4,5-bis(methylsulfonyl)veratrol (**6b**) in different conformations were optimized by minimization of the energy with respect to all the geometrical parameters, thus leading to the global minimum ( $\lambda$ -**6b**, Fig. 12). In this particular conformation, the two *ortho*-positioned sulfonyl groups adopted the characteristic ‘up-and-down’ arrangement –

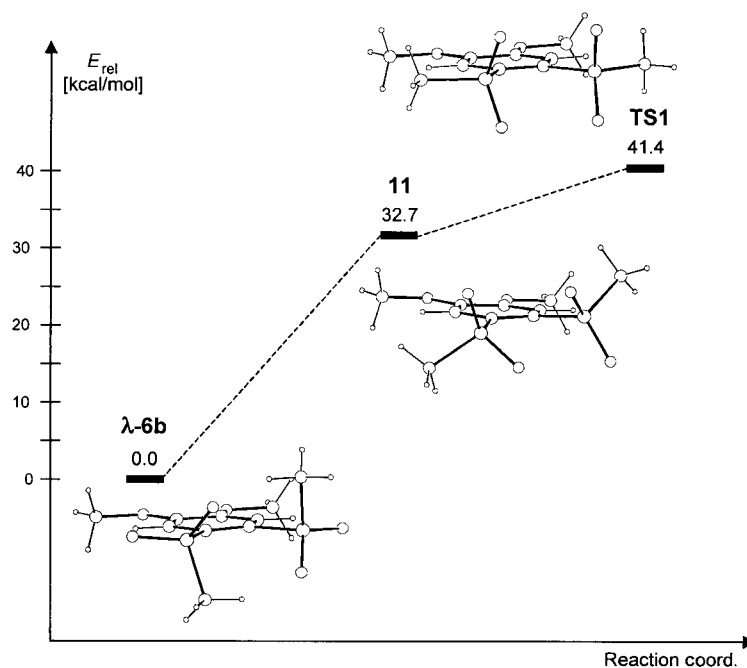
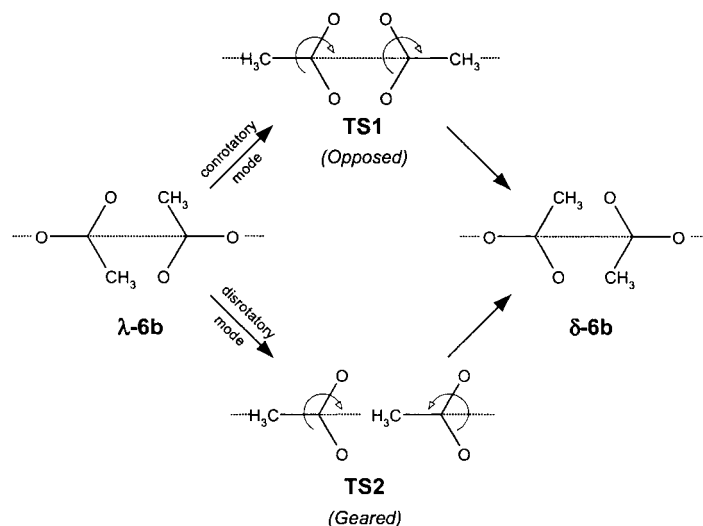


Fig. 12. Schematic B3LYP/3-21G potential-energy surface for the rotational barrier of the sulfonyl groups of **6b** and optimized molecular structures for key stationary points

observed also in the X-ray structure. Extended investigations of the potential-energy surface for the internal rotation of the sulfonyl groups were also undertaken. In the initial step, the potential-energy-surface scan for the internal rotation about the C–S bonds was performed by imposing the C(3)–C(2)–S(2)–C(10) and C(6)–C(1)–S(1)–C(9) dihedral angles (for atom numbering, see Fig. 5) at the regular increments. The reaction coordinate started from the initial value of  $110.8^\circ$  corresponding to the equilibrium geometry of conformer  $\lambda$ -**6b**, and was incrementally decreased to  $0^\circ$ . As shown in Scheme 5, the same dihedral-angle deformation imposed to both sulfonyl groups results in their conrotatory movement. At each of the fixed dihedral angles, the full geometry optimization was performed. The minimum-energy reaction path thus established led eventually to an additional local minimum where the C(3)–C(2)–S(2)–C(10) and C(6)–C(1)–S(1)–C(9) dihedral angles decreased to  $34.7^\circ$ . The optimized geometry projection of this new rotamer **11** is shown in Fig. 12, and its relative energy is  $32.7 \text{ kcal} \cdot \text{mol}^{-1}$  higher when compared to the global minimum of  $\lambda$ -**6b**.

The rotamer corresponding to the highest point of the minimum energy profile was used to locate the *opposed* conformer of the transition state **TS1** for the veratrol **6b** racemization (Scheme 5 and Fig. 12). The vibrational-frequency analysis of **TS1** confirmed the presence of a unique imaginary frequency: a necessary condition for the characterization of transition states. We also undertook the investigation of the

Scheme 5. *Conrotatory and Disrotatory Mode for the Conformational Isomerism in 4,5-Bis(sulfonyl)veratrols*

potential-energy surface corresponding to the disrotatory mode of isomerization *via* the *gearing* transition state **TS2** (Scheme 5). However, for this pathway, we were not able to locate any stationary point at this level of theory<sup>8)</sup>.

The intrinsic-reaction-coordinate calculations (IRC) [15] were initiated from the **TS1** to ensure that the rotamer **11** is connected to this saddle point. The main geometry deformation along this intrinsic reaction coordinate appears to follow the conrotatory movement of the sulfonyl groups. It is noteworthy that, during the IRC procedure, we did not restrict any geometry parameters explicitly. The IRC eventually reached the local minimum **11**, and the investigation was not pursued beyond this point. Indeed, it was obvious from the previously established minimum-energy reaction path that the local minimum **11** and the global minimum  $\lambda\text{-6b}$  are connected on the potential-energy surface *via* the internal rotation of the sulfonyl groups. The schematic coordinate diagram for the barrier to internal rotation of veratrol  $\lambda\text{-6b}$  is summarized in Fig. 12. This barrier amounts to  $41.4 \text{ kcal} \cdot \text{mol}^{-1}$  as computed by the B3LYP/3-21G method. Clearly, this barrier is much higher than that observed by NMR for **6c**. While the 3-21G basis set is convenient for exploration of the potential-energy surfaces for molecules having the size of veratrol **6b**, such a modest basis set is not, however, reliable enough for the energy calculations. Therefore, we resorted to use the B3LYP with the 6-31G\* basis set [16] for the energy calculations and geometry optimizations of the key stationary points located previously on the B3LYP/3-21G surface. The geometry of

<sup>8)</sup> In addition to the conrotatory and disrotatory modes of isomerization, it is possible that step-by-step processes can take place. In this case, only one sulfonyl group would rotate at a time. Our preliminary modeling calculations at the semiempirical level indicated, however, that such a reaction proceeds *via* energy barriers higher than those determined for the concerted rotation of the two functional groups.

each stationary point was re-optimized without any restriction, and the vibrational analysis was performed for the transition states. With the larger basis set, the key dihedral angle C(1)–C(2)–S(2)–C(10), which controls the orientation of the methylsulfonyl group, is optimized to  $73.5^\circ$  and  $179.9^\circ$  for the global minimum  $\lambda$ -**6b'** and the transition state **TS1'**, respectively. The optimized geometry parameters of stationary points were generally quite similar for both theory levels. However, with the larger set, the structure optimization of the local minimum **11** resulted in its rearrangement into the global minimum  $\lambda$ -**6b'**. Therefore the energy profile of the veratrol racemization is simplified, as shown in *Fig. 13*. At the B3LYP/6-31G\* level of theory, the barrier to internal rotation of sulfonyl groups amounts to  $22.3 \text{ kcal} \cdot \text{mol}^{-1}$ . This result is in good agreement with the value observed for **6c**. However, it should be repeated that computations were done on the model compound **6b** with methylsulfonyl groups, while the experimental value was observed for the camphorsulfonyl-substituted veratrol **6c**. It should be noted though, that in the conrotatory mode of isomerization (*Scheme 5*), the steric bulk of the alkyl substituent of the sulfonyl group is not the critical factor for the height of the energy barrier for the process.

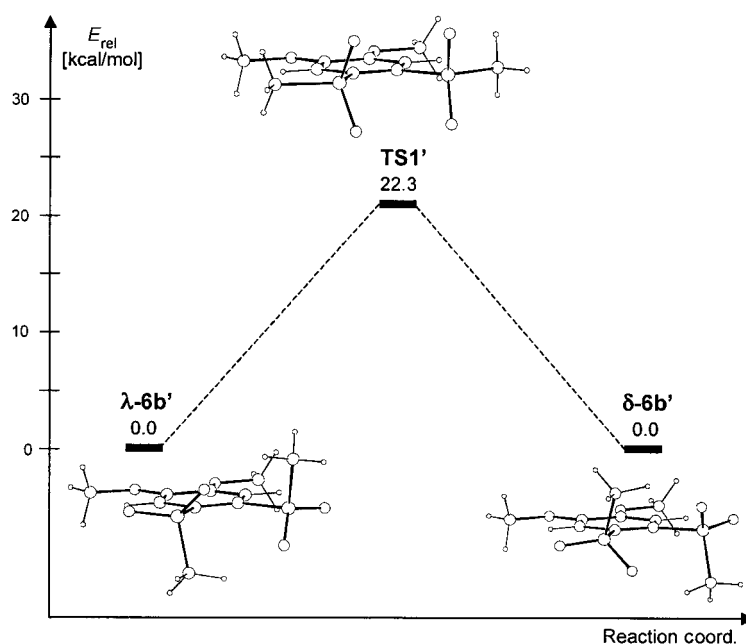


Fig. 13. Schematic B3LYP/6-31G\* potential-energy surface for the conformational isomerism of compound **6b** and optimized molecular structures for key stationary points

**3. Conclusions.** – Aromatic *ortho*-disulfone derivatives (*ortho*-(RSO<sub>2</sub>)<sub>2</sub>Ar) adopt two precise enantiomeric conformations in solution that can be detected by the formation of chiral hexacoordinated tris[4,5-bis(sulfonyl)benzene-1,2-diolato]phosphate anions or camphorsulfonyl derivatives. The rate of conformer interconversion is

slow on the NMR time scale and seems to depend upon the nature of the sulfonyl side chains  $\text{RSO}_2$  ( $\text{R} = \text{Bu}$ ,  $\Delta G^\ddagger = 17 \text{ kcal} \cdot \text{mol}^{-1}$  [10];  $\text{R} = \text{camphor-10-yl}$ ,  $\Delta G^\ddagger = 19.8 \text{ kcal} \cdot \text{mol}^{-1}$ ;  $\text{R} = p\text{-tolyl}$ ,  $\Delta G^\ddagger > 20 \text{ kcal} \cdot \text{mol}^{-1}$ ).

We thank *Damien Jeannerat* and *Scott Smith (NHMFL)* for their attempts to simulate the NMR stereodynamic, as well as the *Swiss National Science Foundation*, the *Federal Office for Education and Science (COST D11)*, the *Société Académique de Genève* for financial support, and the *Fondation de Famille Sandoz (J. L.)*.

### Experimental Part

*General.* Solvents and chemicals are used without purification unless indicated. Toluene was distilled from Na metal, and MeOH, hexane, and  $\text{CH}_2\text{Cl}_2$  from calcium hydride. Dimethylformamide (DMF) was distilled from  $\text{MgSO}_4$  under vacuum and stored over 4 Å molecular sieves under  $\text{N}_2$ .  $\text{CHCl}_3$  (Fluka) and  $\text{CDCl}_3$  were filtered through a plug of basic alumina prior to use. Flash chromatography (FC): pressure 0.1–0.2 bar; *J. T. Baker* silica gel (30–60  $\mu\text{m}$ , 230–400 mesh) or *Fluka* neutral alumina type 507C (100–125 mesh). Anal. gas chromatography (GC): *Hewlett-Packard-HP6890* chromatograph; 30 m  $\times$  0.32 mm nonpolar column (95% dimethylpolysiloxane/5% diphenylpolysiloxane, 0.25  $\mu\text{m}$ ) from *Alltech (HP5)*; classical conditions: 80° for 2 min, then 5°/min, 180° for 5 min;  $t_{\text{R}}$  in min. M.p.: in open capillary tubes; *Stuart-Scientific SMP3* melting-point apparatus; uncorrected. IR Spectra: *Perkin-Elmer 1600* FT-IR spectrophotometer, with KBr. NMR Spectra: *Bruker AMX-400* and *Varian XL-200* spectrometers; at r.t., unless otherwise specified; chemical shift  $\delta$  in ppm from internal standard ( $\text{SiMe}_4$  for  $\delta(\text{H})$  and  $\delta(\text{C})$ ,  $\text{H}_3\text{PO}_4$  for  $\delta(\text{P})$ ), coupling constants  $J$  in Hz. MS: for electrospray (ES), *Finnigan SSQ-7000* spectrometer, for electron ionization (EI) *Varian CH4* or *SMI* spectrometer; in  $m/z$  (rel. %).

1. *4,5-Diiodoveratrol (=1,2-Diiodo-4,5-dimethoxybenzene; 5)*. A soln. of  $\text{H}_5\text{IO}_6$  (2.9 g, 12.8 mmol, 1.0 equiv.) in MeOH (19.0 ml) was stirred for 15 min at 20°.  $\text{I}_2$  (6.4 g, 25.1 mmol, 2.0 equiv.) was then added and the mixture stirred vigorously for 10 min. Veratrol (=1,2-dimethoxybenzene; 4.0 ml, 31.4 mmol, 2.5 equiv.) was added, and the mixture was stirred for 4 h at 70° ( $\rightarrow$  important white precipitate). The hot mixture was then poured into a diluted sodium pyrosulfite soln., and the white solid formed was collected by filtration over a *Büchner* funnel and washed with MeOH. The resulting product was then dissolved in AcOEt and the soln. dried ( $\text{Na}_2\text{SO}_4$ ) and evaporated: 11.5 g (29.4 mmol, 94%) of **5**. No further purification was required. GC:  $t_{\text{R}}$  8.19. M.p. 133° (AcOEt/cyclohexane).  $^1\text{H-NMR}$  ( $\text{CDCl}_3$ , 200 MHz): 7.21 (s, 2 H); 3.81 (s, 6 H).  $^{13}\text{C-NMR}$  ( $\text{CDCl}_3$ , 50 MHz): 149.6; 121.6; 96.0; 56.1. EI-MS (70 eV): 390 (8,  $M^+$ ), 264 (100), 249 (23). HR-MS: 389.86205 ( $\text{C}_8\text{H}_8\text{I}_2\text{O}_2^+$ ; calc. 389.86139).

2. *Sodium Methanesulfinate*. A soln. of sodium sulfite (5.0 g, 39.6 mmol, 1.0 equiv.) in  $\text{H}_2\text{O}$  (19.0 ml) was vigorously stirred for 10 min at 20°.  $\text{NaHCO}_3$  (6.8 g, 81.4 mmol, 2.0 equiv.) was added, and the mixture was stirred for 1 h at 50°. Methanesulfonyl chloride (3.0 ml, 39.2 mmol, 1.0 equiv.) was carefully added, and after the addition, the mixture was vigorously stirred at 50° for 4 h. After cooling to 20°, the  $\text{H}_2\text{O}$  was evaporated for several h. MeOH (5.0 ml) was added to the white residue to separate the sodium methanesulfinate from MeOH-insoluble salts, and the mixture was stirred overnight. Filtration and evaporation gave 3.7 g (94%) of the title product. IR (KBr): 1040–960s ( $\text{SO}_2^-$ ).  $^1\text{H-NMR}$  ( $\text{CD}_3\text{OD}$ , 200 MHz): 2.71.  $^{13}\text{C-NMR}$  ( $\text{CD}_3\text{OD}$ , 50 MHz): 49.63.

3. *Sodium Camphor-10-sulfinate (=Sodium (1S,4R)-7,7-Dimethyl-2-oxobicyclo[2.2.1]heptane-1-methanesulfinate; 10)*. As described for sodium methanesulfinate, from sodium sulfite (750 mg, 6.0 mmol, 1.0 equiv.) in  $\text{H}_2\text{O}$  (9.0 ml),  $\text{NaHCO}_3$  (1.0 g, 12.0 mmol, 2.0 equiv.), and (+)-camphor-10-sulfonyl chloride (= (1S,4R)-7,7-dimethyl-2-oxobicyclo[2.2.1]heptane-1-methanesulfonyl chloride; 1.4 g, 5.7 mmol, 0.9 equiv.): 1.4 g (100%) of **10**. IR (KBr): 1040–960s ( $\text{SO}_2^-$ ).  $^1\text{H-NMR}$  ( $\text{CD}_3\text{OD}$ , 400 MHz): 2.40–2.26 (m, 2 H); 2.16 (dd,  $J = 191, 13, 2 \text{ Hz}$ ); 2.10–1.99 (m, 2 H); 1.87 (d,  $J = 18, 1 \text{ Hz}$ ); 1.60–1.53 (m, 1 H); 1.46–1.40 (m, 1 H); 1.06 (s, 3 H); 0.90 (s, 3 H).  $^{13}\text{C-NMR}$  ( $\text{CD}_3\text{OD}$ , 100 MHz): 218.3; 60.2; 58.4; 42.7; 42.4; 26.5; 25.5; 18.8; 18.7.

4. *4,5-Bis(p-tolylsulfonyl)veratrol (=1,2-Dimethoxy-4,5-bis[(4-methylphenyl)sulfonyl]benzene; 6a)*. A soln. of **5** (3.3 g, 8.5 mmol, 1.0 equiv.) in freshly distilled DMF (from  $\text{MgSO}_4$ ; 67.0 ml) was vigorously stirred under Ar for 10 min at 20°. CuI (5.0 g, 26.2 mmol, 3.0 equiv.) was added, and the mixture was stirred for 10 min. Sodium 4-methylbenzenesulfinate (5.0 g, 28.1 mmol, 3.3 equiv.) was added and the mixture was vigorously stirred under Ar for 72 h at 110°. The mixture was allowed to cool to 20° and diluted with  $\text{H}_2\text{O}$  (100.0 ml) and AcOEt (100.0 ml). The precipitate formed was removed by filtration over a *Büchner* funnel. The org. layer was

washed with H<sub>2</sub>O (2 × 70.0 ml) and sat. NaHCO<sub>3</sub> soln. (2 × 50.0 ml), dried (Na<sub>2</sub>SO<sub>4</sub>), and evaporated: 3.0 g (88%) of **6a**. Recrystallization from AcOEt/hexane gave **6a**. White needles. GC: *t<sub>R</sub>* 9.66. M.p.: 193–194° (AcOEt/cyclohexane). <sup>1</sup>H-NMR (CDCl<sub>3</sub>, 200 MHz): 7.91 (s, 2 H); 7.81 (d, *J* = 4, 4 H); 7.27 (d, *J* = 4, 4 H); 4.03 (s, 6 H); 2.39 (s, 6 H). <sup>13</sup>C-NMR (CDCl<sub>3</sub>, 50 MHz): 151.9; 143.9; 139.2; 133.0; 129.3; 127.8; 115.3; 56.8; 21.6. EI-MS (70 eV): 446 (100, *M*<sup>+</sup>), 414 (31); 382 (70), 243 (60), 212 (59), 139 (73), 91 (89). HR-MS: 446.08817 (C<sub>22</sub>H<sub>22</sub>O<sub>6</sub>S<sub>2</sub><sup>+</sup>; calc. 446.08578).

5. 4,5-Bis(methylsulfonyl)veratrol (= 1,2-Dimethoxy-4,5-bis(methylsulfonyl)benzene; **6b**). As described for **6a** (Exper. 4), from **5** (1.0 g, 2.6 mmol, 1.0 equiv.), DMF (21.0 ml), CuI (1.5 g, 7.7 mmol, 3.0 equiv.), and sodium methanesulfinate (786 mg, 7.7 mmol, 3.0 equiv.): 750 mg (2.6 mmol, 100%) of **6b**. Recrystallization from AcOEt/cyclohexane gave **6b**. Colorless rectangular crystals. GC: *t<sub>R</sub>* 9.71. M.p. 222–224° (AcOEt/cyclohexane). <sup>1</sup>H-NMR (CDCl<sub>3</sub>, 200 MHz): 7.76 (s, 2 H); 4.02 (s, 6 H); 3.42 (s, 6 H). <sup>13</sup>C-NMR (CDCl<sub>3</sub>, 50 MHz): 114.6; 56.8; 45.6. EI-MS (70 eV): 294 (100, *M*<sup>+</sup>), 169 (61), 140 (27), 79 (7), 63 (10). HR-MS: 294.02109 (C<sub>10</sub>H<sub>14</sub>O<sub>6</sub>S<sub>2</sub><sup>+</sup>; calc. 294.02319).

*X-Ray Crystal Structure of 6b*. C<sub>10</sub>H<sub>14</sub>O<sub>6</sub>S<sub>2</sub>, *M<sub>r</sub>* 294.3;  $\mu = 3.830 \text{ mm}^{-1}$ ,  $d_x = 1.477 \text{ g} \cdot \text{cm}^{-3}$ , monoclinic, *P*2<sub>1</sub>/*c*, *Z* = 4, *a* = 7.5870(3), *b* = 8.5460(7), *c* = 20.417(1) Å,  $\beta = 90.923(3)^\circ$ , *V* = 1323.6(3) Å<sup>3</sup>; colourless prism 0.15 × 0.18 × 0.29 mm. Cell dimensions and intensities were measured at r.t. on a *Stoe Stadi4* diffractometer with graphite-monochromated Cu[K $\alpha$ ] radiation ( $\lambda = 1.5418 \text{ \AA}$ ),  $\omega$ -2 $\theta$  scans, scan width 1.05° + 0.35 tg  $\theta$ , and scan speed 0.06°/s. Two reference reflections measured every 45 min showed no variation.  $-7 < h < 7$ ;  $0 < k < 8$ ;  $0 < l < 21$ . The structure was solved by direct methods [17]. Measured reflections, 1658; unique reflections, 1605, of which 1277 were observables ( $|F_o| > 4\sigma(F_o)$ ); *R<sub>int</sub>* = 0.030. Data were corrected for Lorentz and polarization effects and for absorption [18] (*T<sub>min,max</sub>* = 0.43306, 62375). All calculations were performed with the XTAL system [19]. Full-matrix least-squares refinement based on *F* with a weight of  $1/(\sigma^2(F_o) + 0.00012(F_o)^2)$  gave the final values *R* = 0.044,  $\omega R$  = 0.042, and *S* = 1.97(4) for 206 variables and 1277 contributing reflections. The maximum shift/error on the last cycle was  $0.56 \cdot 10^{-2}$ . The final difference electron-density map showed a maximum of +0.27 and a minimum of  $-0.30 \text{ e} \cdot \text{\AA}^{-3}$ . H-Atoms of the Me substituents were refined with restraints on bond lengths and bond angles and both aromatic H-atoms were refined without restraint.

Crystallographic data for **6b** (excluding structure factors) have been deposited with the Cambridge Crystallographic Data Center (deposition N° CCDC 178337). Copies of the data can be obtained, free of charge, on application to the CCDC, 12 Union Road, Cambridge CB2 1EZ, UK (fax: +44(1223)336-033; e-mail: deposit@ccdc.cam.ac.uk).

6. 4,5-Bis(camphor-10-sulfonyl)veratrol (= 1,2-Bis[[(1*S*,4*R*)-7,7-dimethyl-2-oxobicyclo[2.2.1]hept-1-yl]-methylsulfonyl]-4,5-dimethoxybenzene; **6c**). As described for **6a** (Exper. 4), from **5** (299 mg, 0.7 mmol, 1.0 equiv.), DMF (31.0 ml), CuI (432 mg, 2.3 mmol, 3.0 equiv.), and **10** (4.5 g, 19.1 mmol, 25.0 equiv.): 370 mg (0.7 mmol, 85%) of **6c** as a brown oil, which was purified by FC (SiO<sub>2</sub>, AcOEt/cyclohexane 1:1): pale yellow oil. GC: *t<sub>R</sub>* 2.95. <sup>1</sup>H-NMR (CDCl<sub>3</sub>, 400 MHz; (*m*) = minor; (*M*) = major): 8.27 (s, 2 H (*m*)); 8.1827 (s, 2 H (*M*)); 5.19 (d, *J* = 14.3, 2 H (*m*)); 4.98 (d, *J* = 14.2, 2 H (*M*)); 4.64 (d, *J* = 14.3, 2 H (*m*)); 4.63 (d, *J* = 14.2, 2 H (*M*)); 3.27 (s, 6 H (*M*)); 3.56 (d, *J* = 14.9, 2 H (*M*)); 3.36 (d, *J* = 15.4, 2 H (*m*)); 2.90 (d, *J* = 14.9, 2 H (*M*)); 2.79 (d, *J* = 15.4, 2 H (*m*)); 3.15 (s, 6 H (*m*)); 2.43–1.43 (*m*, 10 H); 1.04 (s, 6 H (*M*)); 1.03 (s, 6 H (*m*)); 0.90 (s, 6 H (*m*)); 0.89 (s, 6 H (*M*)). <sup>13</sup>C-NMR (CDCl<sub>3</sub>, 100 MHz): 216.4 (*m*); 214.3 (*M*); 163.6; 162.9; 162.4; 70.8 (*m*); 65.6 (*M*); 60.3; 59.4 (*m*); 58.9 (*M*); 51.4 (*M*); 50.1 (*m*); 49.1 (*m*); 48.5 (*M*); 42.5; 36.6 (*m*); 35.9 (*M*); 32.3 (*M*); 31.5 (*m*); 27.0 (*M*); 26.8 (*m*); 26.1 (*m*); 25.5 (*M*); 19.7; 19.5 (*M*); 19.3 (*m*). EI-MS (70 eV): 566 (2, *M*<sup>+</sup>), 534 (100), 502 (21), 216 (45), 151 (53).

7. 4,5-Bis(*p*-tolylsulfonyl)pyrocatechol (= 4,5-Bis[(4-methylphenyl)sulfonyl]benzene-1,2-diol; **7a**). A soln. of **6a** (1.8 g, 3.9 mmol, 1.0 equiv.) in CH<sub>2</sub>Cl<sub>2</sub> (80.0 ml) was stirred under Ar for 10 min at 20°. BBr<sub>3</sub> (2.4 ml, 19.7 mmol, 5.0 equiv.) was then slowly and carefully added, and the mixture was vigorously stirred at 45° during 16 h. The mixture was allowed to cool to 0°, and H<sub>2</sub>O was carefully added. The org. layer was washed with 10% HCl soln. (2 × 50 ml), dried (Na<sub>2</sub>SO<sub>4</sub>), and evaporated: 1.5 g (93%) of **7a**. GC: *t<sub>R</sub>* 9.43. <sup>1</sup>H-NMR (CDCl<sub>3</sub>, 200 MHz): 7.98 (s, 2 H); 7.78–7.74 (d, *J* = 4, 4 H); 7.49 (s, 2 H); 7.24–7.20 (d, *J* = 4, 4 H); 2.35 (s, 6 H). <sup>13</sup>C-NMR (CDCl<sub>3</sub>, 50 MHz): 147.2; 144.2; 138.7; 131.9; 129.4; 127.7; 120.1; 21.6. EI-MS (70 eV): 418 (15, *M*<sup>+</sup>), 354 (11), 264 (53), 156 (17), 155 (30), 108 (37), 91 (100), 65 (37). HR-MS: 418.05277 (C<sub>20</sub>H<sub>18</sub>O<sub>6</sub>S<sub>2</sub><sup>+</sup>; calc. 418.05447).

8. 4,5-Bis(methylsulfonyl)pyrocatechol (= 4,5-Bis(methylsulfonyl)benzene-1,2-diol; **7b**). As described for **7a** (Exper. 7), from **6b** (475 mg, 1.6 mmol, 1.0 equiv.), CH<sub>2</sub>Cl<sub>2</sub> (26.5 ml), and BBr<sub>3</sub> (1.0 ml, 8.2 mmol, 5 equiv.) at 20° for 16 h: 430 mg (1.6 mmol, 100%) of **7b**. Recrystallization from acetone/hexane gave **7b**. White solid. GC: *t<sub>R</sub>* 9.66. M.p.: 265° (dec.; acetone/hexane). <sup>1</sup>H-NMR ((D)<sub>6</sub>acetone, 200 MHz): 9.60 (s, 2 H); 7.72 (s, 2 H); 3.36 (s, 6 H). <sup>13</sup>C-NMR ((D)<sub>6</sub>acetone, 100 MHz): 149.8; 132.7; 120.6; 45.5. EI-MS (70 eV): 266 (100, *M*<sup>+</sup>), 203 (46), 187 (23), 141 (39), 125 (46), 79 (49), 63 (55). HR-MS: 265.99112 (C<sub>8</sub>H<sub>10</sub>O<sub>6</sub>S<sub>2</sub><sup>+</sup>; calc. 265.99188).

9. *Bis[4-(dimethylamino)phenyl]phenylmethylium Tris[4,5-bis[(4-methylphenyl)sulfonyl]benzenediolato(2-)-κO,κO']phosphate(1-)* (**8·3a**). In a flame-dried flask under N<sub>2</sub> (addition funnel for solid and reflux condenser topped with a gas outlet connected to a trap of conc. NaOH soln.), a soln. of **7a** (35 mg, 83 μmol, 3.0 equiv.) in CH<sub>2</sub>Cl<sub>2</sub> (1.0 ml) was stirred for 10 min at r.t. PCl<sub>5</sub> (6 mg, 27 μmol, 1.0 equiv.) was added and the mixture stirred for 10 min at r.t. The CH<sub>2</sub>Cl<sub>2</sub> was then evaporated, the DMF (1.0 ml) added and the mixture stirred for 12 h at r.t. Then Bu<sub>3</sub>N (6.5 μl, 27 μmol, 1.0 equiv.) was added. After 8 h of additional stirring at 25°, the solvent was evaporated and the resulting brown oil purified by cation exchange with malachite green in CH<sub>2</sub>Cl<sub>2</sub> followed by FC (SiO<sub>2</sub>, CH<sub>2</sub>Cl<sub>2</sub>): **8·3a** (27.5 mg, 63%). Deep green oil. <sup>1</sup>H-NMR ((D)<sub>6</sub>DMSO, 400 MHz): 8.07 (br. s, 2 H); 8.00 (s, 6 H); 7.83 (br. d, *J* = 8.3, 16 H); 7.75 (br. d, *J* = 1.8, 4 H); 7.34 (br. d, *J* = 9.1, 4 H); 7.30–7.26 (*m*, 17 H); 6.83 (*d*, *J* = 9.1, 4 H); 3.21 (*s*, 12 H); 2.42 (*s*, 18 H). <sup>13</sup>C-NMR ((D)<sub>6</sub>DMSO, 100 MHz): 155.5; 148.3; 148.2; 148.0; 143.7; 143.4; 139.7; 139.4; 139.2; 132.7; 131.9; 129.2; 129.1; 127.9; 127.7; 126.6; 120.2; 114.6; 114.4; 112.3; 77.2; 40.3; 21.5. <sup>31</sup>P-NMR ((D)<sub>6</sub>DMSO, 162 MHz): –76.72; –77.34; –77.53; –78.23. ES-MS: pos. mode: 329 (100); neg. mode: 1279 (36), 1115 (100); 141 (39), 125 (46), 79 (49), 63 (55).

10. *Bis[4-(dimethylamino)phenyl]phenylmethylium Tris[4,5-bis(methylsulfonyl)benzenediolato(2-)-κO,κO']phosphate(1-)* (**8·3b**). As described for **8·3a** (*Exper.* 9), from **7b** (100 mg, 375 μmol, 3.0 equiv.) in MeCN (8.0 ml), PCl<sub>5</sub> (26 mg, 125 μmol, 1.0 equiv.), then in DMF (8.0 ml) with Bu<sub>3</sub>N (30 μl, 124 μmol, 1.0 equiv.). Of the crude pale yellow oil (188 mg), an aliquot (24 mg, 24 μmol, 1.0 equiv.) was purified by cation exchange with malachite green (24.5 mg, 26 μmol, 1.1 equiv.) in CH<sub>2</sub>Cl<sub>2</sub>/acetone 1:2 (3 ml), followed by FC (SiO<sub>2</sub>, CH<sub>2</sub>Cl<sub>2</sub>/AcOEt 8:2): **8·3b** (15 mg, 55%). This corresponds to an overall yield of 82%. Deep green oil. <sup>1</sup>H-NMR ((D)<sub>6</sub>acetone, 400 MHz): 7.77–7.74 (*m*, 1 H); 7.67 (br. s, 1 H); 7.64–7.60 (*m*, 2 H); 7.53–7.52 (*m*, 5 H); 7.44–7.38 (*m*, 6 H); 7.10 (*d*, *J* = 9.6, 4 H); 3.38 (br. s, 12 H); 3.36 (br. s, 18 H). <sup>13</sup>C-NMR ((D)<sub>6</sub>acetone, 100 MHz): 157.0; 148.5 (*d*, <sup>2</sup>*J*(C,P) = 5.0); 140.6; 134.4; 133.0; 132.9; 128.5; 127.0; 119.6; 113.6; 113.2 (*d*, <sup>3</sup>*J*(C,P) = 17.4); 59.5; 44.6; 40.1. <sup>31</sup>P-NMR ((D)<sub>6</sub>acetone, 162 MHz): –76.16. ES-MS: pos. mode: 329 (100); neg. mode: 823 (36), 539 (42), 265 (36), 173 (39), 113 (88), 95 (100).

## REFERENCES

- [1] A. Von Zelewsky, 'Stereochemistry of Coordination Compounds', John Wiley & Sons, Chichester, UK, 1996.
- [2] J. Lacour, C. Ginglinger, C. Grivet, G. Bernardinelli, *Angew. Chem., Int. Ed.* **1997**, *36*, 608; J. Lacour, C. Ginglinger, F. Favarger, *Tetrahedron Lett.* **1998**, 4825.
- [3] J. Lacour, C. Ginglinger, F. Favarger, S. Torche-Haldimann, *Chem. Commun.* **1997**, 2285; J. Lacour, S. Torche-Haldimann, J. J. Jodry, C. Ginglinger, F. Favarger, *Chem. Commun.* **1998**, 1733; J. Lacour, J. J. Jodry, C. Ginglinger, S. Torche-Haldimann, *Angew. Chem., Int. Ed.* **1998**, *37*, 2379; J. Lacour, C. Goujon-Ginglinger, S. Torche-Haldimann, J. J. Jodry, *Angew. Chem., Int. Ed.* **2000**, *39*, 3695; H. Ratni, J. J. Jodry, J. Lacour, E. P. Kündig, *Organometallics* **2000**, *19*, 3997; J. Giner Planas, D. Prim, F. Rose-Munch, E. Rose, D. Monchaud, J. Lacour, *Organometallics* **2001**, *20*, 4107.
- [4] C. Hansh, A. Leo, R. W. Taft, *Chem. Rev.* **1991**, *91*, 165; J. Borgulya, K. Bernauer, G. Zürcher, M. Da Prada, *Helv. Chim. Acta* **1989**, *72*, 952.
- [5] H. Suzuki, H. Abe, *Tetrahedron Lett.* **1995**, *36*, 6239.
- [6] J. Wisniewski Grissom, G. U. Gunawardena, *Tetrahedron Lett.* **1995**, *36*, 4951; H. Suzuki, K. Nakamura, R. Goto, *Bull. Chem. Soc. Jpn.* **1966**, *39*, 128.
- [7] L. O. Farnig, J. L. Kice, *J. Am. Chem. Soc.* **1981**, *103*, 1137; E. Krauthausen, in 'Organosulfur Compounds', Vol. E11, Ed. D. Klamann, Georg Thieme Verlag, Stuttgart, 1985, p. 619.
- [8] J. F. W. McOmie, M. L. Watts, D. E. West, *Tetrahedron* **1968**, *24*, 2289.
- [9] E. J. Corey, J. C. Bailar Jr., *J. Am. Chem. Soc.* **1959**, *81*, 2620.
- [10] D. M. Collard, M. J. Sadri, D. VanDerveer, K. S. Hagen, *J. Chem. Soc., Chem. Commun.* **1995**, 1357.
- [11] J. Lacour, D. Monchaud, G. Bernardinelli, F. Favarger, *Org. Lett.* **2001**, *3*, 1407.
- [12] A. D. Becke, *J. Chem. Phys.* **1993**, *98*, 5648; C. Lee, W. Yang, R. G. Parr, *Phys. Rev. B* **1988**, *37*, 785; B. Miehlich, A. Savin, H. Stoll, H. Preuss, *Chem. Phys. Lett.* **1989**, *157*, 200.
- [13] J. S. Binkley, J. A. Pople, W. J. Hehre, *J. Am. Chem. Soc.* **1980**, *102*, 939; K. D. Dobbs, W. J. Hehre, *J. Comput. Chem.* **1987**, *8*, 880.
- [14] M. J. Frisch, G. W. Trucks, H. B. Schlegel, G. E. Scuseria, M. A. Robb, J. R. Cheeseman, V. G. Zakrzewski, J. A. Montgomery, R. E. Stratmann, J. C. Burant, S. Dapprich, J. M. Millam, A. D. Daniels, K. N. Kudin, M. C. Strain, O. Farkas, J. Tomasi, V. Barone, M. Cossi, R. Cammi, B. Mennucci, C. Pomelli, C. Adamo, S.



- Clifford, J. Ochterski, G. A. Petersson, P. Y. Ayala, Q. Cui, K. Morokuma, D. K. Malick, A. D. Rabuck, K. Raghavachari, J. B. Foresman, J. Cioslowski, J. V. Ortiz, B. B. Stefanov, G. Liu, A. Liashenko, P. Piskorz, I. Komaromi, R. Gomperts, R. L. Martin, D. J. Fox, T. Keith, M. A. Al-Laham, C. Y. Peng, A. Nanayakkara, C. Gonzalez, M. Challacombe, P. M. W. Gill, B. G. Johnson, W. Chen, M. W. Wong, J. L. Andres, M. Head-Gordon, E. S. Replogle, J. A. Pople, 'Gaussian 98 (Revision A.7)', Gaussian, Inc., Pittsburgh PA, 1998.
- [15] C. Gonzalez, H. B. Schlegel, *J. Chem. Phys.* **1989**, *90*, 2154; C. Gonzalez, H. B. Schlegel, *J. Phys. Chem.* **1990**, *94*, 5523.
- [16] R. Ditchfield, W. J. Hehre, J. A. Pople, *J. Chem. Phys.* **1971**, *54*, 724; M. S. Gordon, *Chem. Phys. Lett.* **1980**, *76*, 163.
- [17] P. Main, S. J. Fiske, S. E. Hull, L. Lessinger, G. Germain, J.-P. Declercq, M. M. Woolfson, 'A System of Computer Programs for the Automatic Solution of Crystal Structures from X-Ray Diffraction Data', Univs. of York, England, and Louvain-la-Neuve, Belgium, 1987.
- [18] E. Blanc, D. Schwarzenbach, H. D. Flack, *J. Appl. Crystallogr.* **1991**, *24*, 1035.
- [19] 'XTAL 3.2 User's Manual', Eds. S. R. Hall, H. D. Flack, J. M. Stewart, Universities of Western Australia and Maryland, 1992.

*Received May 29, 2002*